New Developments on Metallurgy and Applications of High Strength Steels, Buenos Aires 2008, Argentina

STRONG BAINITIC STEELS BY CONTINUOUS COOLING TRANSFORMATION

G. Gomez, T. Pérez and H. K. D. H. Bhadeshia[†]

Department of Metallurgy, Siderca R & D
Simini 250, 2804 Campana
Provincia de Buenos Aires, Argentina

[†]Materials Science and Metallurgy, University of Cambridge
Cambridge CB2 3QZ, U.K.

Keywords: carbide–free, bainite, continuous cooling, alloy design, properties, as–rolled

Abstract

Using metallurgical models, three steels were designed to obtain carbide-free bainitic structures in the as-rolled condition. Experimental castings were hot-rolled in a pilot mill and their austenite decomposition kinetics were measured using dilatometry. Tensile and Charpy impact properties were measured and the microstructures were characterised using X-ray diffractometry, optical and scanning electron microscopy. Promising results were obtained when the microstructure was composed of a fine mixture of bainitic ferrite and retained austenite. In this case, 140 ksi (965 MPa) of yield strength was achieved in combination with good toughness. Conversely, when the structure was coarse with blocks of retained austenite between bainitic sheaves or when large martensitic regions were present, the impact properties were strongly impaired.

1 Introduction

Quenching and tempering is the standard route in the production of strong steels [1–3]. One interesting alternative to get the same or improved mechanical properties avoiding heat treatments [4, 5] using alternative microstructures generated by continuous cooling transformation following hot–processing. It becomes difficult to adopt this route when the strength required is in excess of 1000 MPa whilst maintaining toughness in thick section, but there has been progress in the context of continuously cooled, carbide–free bainitic steels [6–8]. The chemical composition of these steels must be such that the ferrite and pearlite reactions are avoided during air cooling from austenite. The loss of toughness and ductility commonly observed with bainite is related to the presence of coarse cementite particles between the bainitic ferrite sheaves [9]. To avoid this problem, the cementite formation can be inhibited by the addition of about 1.5 wt% of Si or Al [10–24]. These elements do not dissolve in cementite and hence suppress its precipitation [25–27]. The expected as–rolled structure is a fine mixture of ferrite plates and retained interlath austenite that achieves strength without sacrificing toughness.

The purpose of this work was to create a carbide–free bainitic steel with a specified combination of strength and Charpy toughness by continuous cooling from austenite over a range of cooling rates consistent with industrial processing. The methodology is partly based on the procedures described in [6–8].

2 Alloy design

The objective was to obtain a mixed microstructure consisting of bainitic ferrite and films of retained austenite during air cooling from the austenitic range. From calculations performed with a finite element thermal model it was estimated that for material thicknesses between 24 mm and 6 mm, the average cooling rate at the exit of the hot–rolling mill used, for a rolling temperature in the range 1100-950°C, is between 0.1–$0.5^{\circ}\mathrm{C\,s^{-1}}$. Three alloys were designed both to achieve the desired microstructure within the processing range and to assess the methodology used to design the alloys. The concentration of each element was selected with the aid of a metallurgical model for the calculation of time–temperature–transformation (TTT) diagrams [28–31]. The resulting specifications of the alloys are listed in Table 1.

Table 1: Chemical compositions (wt%) of the steels used.

	Alloy 1		Alloy 2		Alloy 3	
	Specified	Actual	Specified	Actual	Specified	Actual
C	0.25	0.24	0.30	0.30	0.35	0.32
Mn	0.10	0.09	0.10	0.10	0.60	0.61
Si	1.40	1.27	1.40	1.42	0.30	0.30
Cr	1.00	1.00	1.00	1.03	1.70	1.74
Mo	0.25	0.23	0.25	0.22	0.25	0.25
Ni	3.6	3.64	3.6	3.48	3.6	3.58
Al	0.03	0.014	0.03	0.040	1.20	1.25

Alloys 1 and 2 differed only in the carbon concentration, to enable its significance on the microstructure and properties to be quantified. Alloy 3 in contrast was significantly different, with the largest carbon concentration to enhance microstructural refinement, and silicon substantially replaced with aluminium as the cementite inhibiting solute. Since aluminium also increases the free energy of transformation of austenite to ferrite, the hardenability had to be adjusted with the help of larger manganese and chromium additions.

The role of the solutes can be summarised as follows:

- Carbon to depress the bainite–start temperature (B_S), and hence to refine of the microstructure [32–38].
- Silicon and aluminium both inhibit the precipitation of cementite so that the carbon that is partitioned into the austenite remains there and is retained at room temperature.
- Chromium, molybdenum and nickel all enhance hardenability. Molybdenum also enhances resistance to temper embrittlement [39, 40].
- Manganese enhances hardenability but its concentration must be kept to a minimum to avoid banded microstructures [41, 42] and avoid blocky regions of retained austenite [43, 44].

Kinetic calculations using the metallurgical model [28–31] indicated that all three alloys would present a mainly bainitic microstructure after cooling at 0.1-0.5$^\circ\mathrm{C\,s^{-1}}$. At the lower end of this range some allotriomorphic ferrite was expected to form but the fraction obtained was only 0.05 due to the sluggish reaction kinetics. Conversely, martensite was expected for cooling at rates higher than 0.5$^\circ\mathrm{C\,s^{-1}}$. Its maximum amount was difficult to estimate due to uncertainties in the calculation of the bainite reaction kinetics.

On the basis of the calculations, it was expected that the final microstructure would be composed of bainite for cooling rates in the range 0.1–0.5$^\circ\mathrm{C\,s^{-1}}$. The calculated B_S temperatures were 471°C, 446°C and 423°C for Alloys 1, 2 and 3 respectively. A low transformation temperature is conducive to a fine structure capable of achieving high strength without compromising toughness.

3 Experimental

Three alloys were prepared as 20 kg melts in a vacuum induction furnace. The obtained steel chemistries are shown in Table 1. The resulting slabs of 140 mm thickness were hot rolled in a pilot mill to a final thickness of 16 mm. During hot rolling, the reheating and finishing temperatures were 1200–1250°C and 1000–950°C respectively. After hot rolling, the plates were air cooled to room temperature. The as–rolled microstructures were characterised using optical and scanning electron microscopy, Vickers hardness, and X–ray diffractometry.

Standard tensile and Charpy V–notch tests using $10 \times 10 \times 50\,\mathrm{mm}$ samples were conducted on the as–rolled steel. The reported ensile properties represent an average of two repeated tests. Similarly, the impact properties measured at room temperature, 0°C, -20°C and -40°C correspond to averages over three repeated tests for each temperature. The lengths of the Charpy samples were in all cases parallel to the transverse direction of the steel plate (perpendicular to the rolling direction) and the V–notches were machined in the through–thickness direction.

Continuous cooling transformation (CCT) diagrams were determined using a Gleeble thermomechanical simulator. The resulting samples were characterised using optical microscopy and hardness measurements.

4 Continuous Cooling Transformation Diagrams

Measured CCT diagrams are shown in Fig. 1. The samples were heated at 5$^\circ\mathrm{C\,s^{-1}}$ up to 1000° and then immediately cooled without holding at the maximum temperature. The cooling rates used were constant and in the range 0.1–10$^\circ\mathrm{C\,s^{-1}}$. The measured austenite grain size was for all the samples, in the range 40–60 $\mu\mathrm{m}$.

In Fig. 2 shows the hardness values as a function of the cooling rate and alloy. The calculated hardness values [45] of the fully martensitic alloys are represented as horizontal lines.

When comparing the transformation kinetics of Alloys 1 and 2 (Fig. 1, it is evident that the greater carbon concentration of the latter does not significantly influence B_S. There was nevertheless a noticeable reduction in the rate of transformation of Alloy 2l as can be seen in the shift of the fraction–transformed contours to lower temperatures.

Alloy 3 shows peculiar behaviour. With its enhanced Cr and Mn content, the cooling rate necessary to obtain 90% martensite is reduced from $2^\circ\mathrm{C\,s^{-1}}$ in Alloys 1 and 2, to $0.8^\circ\mathrm{C\,s^{-1}}$ in Alloy 3. At the same time, the large aluminium concentration accelerates the early stages of the allotriomorphic ferrite reaction. But in spite of this, at least 80% of the transformation occurs below the calculated $B_S = 324^\circ$C when the material is cooled at 0.1$^\circ\mathrm{C\,s^{-1}}$, so most of the transformation at all cooling rates occurs at low temperatures.

Finally, it is important to note that the full line denoting the M_S temperature is determined from an abrupt change in the slope of the transformation strain versus temperature curve during continuous cooling. Those for Alloys 1 and 2 are not plotted for cooling rates less than 0.5$^\circ\mathrm{C\,s^{-1}}$ because martensitic transformation was absent. In contrast, Alloy 3 always exhibited martensite even down to a cooling rate of 0.1$^\circ\mathrm{C\,s^{-1}}$.

5 As–Rolled Microstructures

Scanning electron micrographs of Alloy 1 in the as–rolled condition are shown in Fig. 3a,b; as expected, they show the mixture of bainitic ferrite and retained austenite. The fraction of austenite was determined using X–ray diffraction a 0.18 ± 0.01, where the error is estimated from Rietveld analysis of the X–ray patterns. Some of the austenite was present in the form of blocks as large as 5 μm in size. The hardness of the microstructure wa 382±5 HV20.

In contrast, the microstructure of Alloy 2 in the as–rolled state seems much finer, Fig. 3c,d. There were also some small regions identified as retained austenite and slightly auto–tempered martensite. The retained austenite content was determined to be 0.13 which is smaller than that of Alloy 1, but few blocky regions of austenite were observed; blocks of austenite are known to be detrimental to toughness [22, 46]. The blocks tend to transform into coarse, high–carbon, untempered and brittle martensite under the influence of stress. The hardness of the microstructure was much higher, 468±5 HV20, a value similar to that obtained after heat–

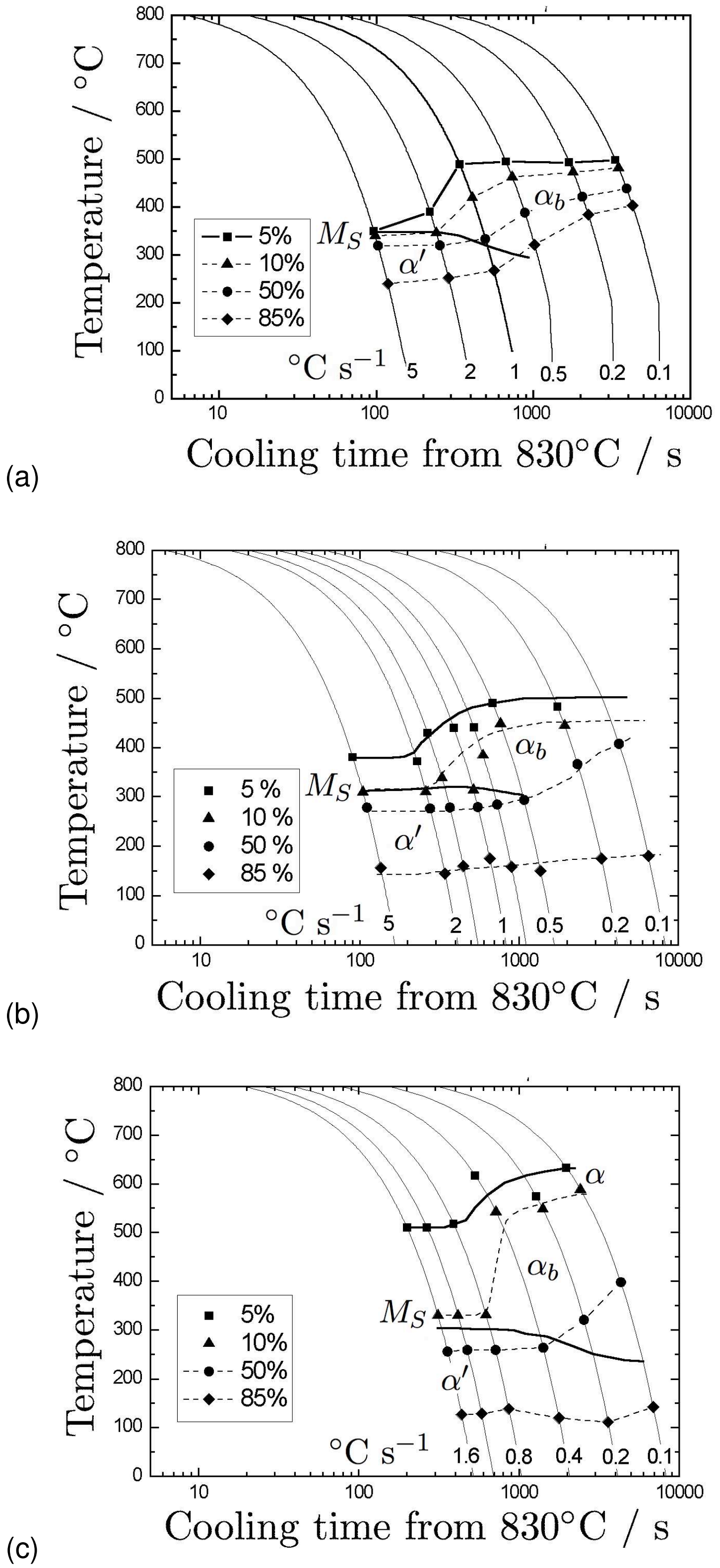

Figure 1: CCT diagrams for samples with an austenite grain size in the range 40–60 μm and austenitisation temperature of 1000°C. (a) Alloy 1. (b) Alloy 2. (c) Alloy 3. The terms α, α_b and α' refer to allotriomorphic ferrite, bainite and martensite respectively.

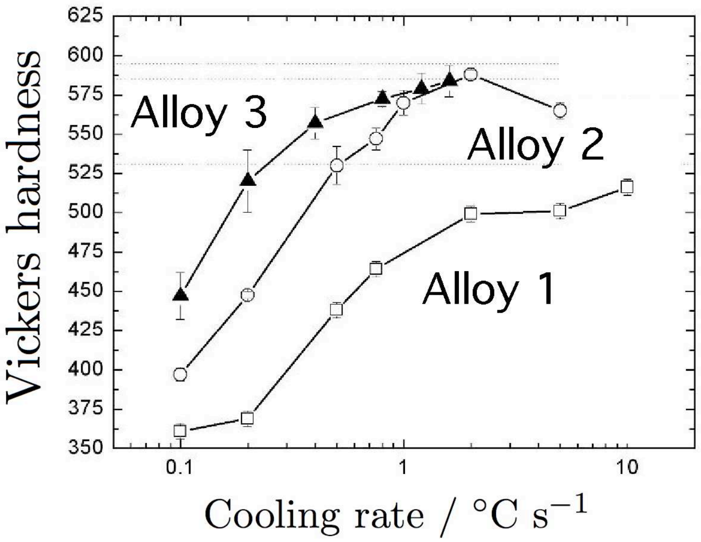

Figure 2: Vickers hardness using a 20 kg load. The horizontal lines represent in ascending order, the hardness values of Alloys 1,2,3 respectively, in their fully martensitic states.

treatment in the Gleeble experiments for a cooling rate of 0.2 $^\circ\mathrm{C\,s^{-1}}$. From this, it is concluded that 0.2 $^\circ\mathrm{C\,s^{-1}}$ was the average cooling rate when the hot 16 mm plates were cooled in air after hot rolling.

The reason why the microstructure of Alloy 2 is refined relative to Alloy 1 is that the transformation temperature is suppressed by the higher carbon concentration. It is well known [32–35] that finer bainite is obtained by transformation at lower temperatures. This also explains the greater hardness obtained.

Fig. 3e,f shows the corresponding micrographs for Alloy 3. The microstructure is fine but there are significant regions of untempered martensite which will have a high carbon concentration due to the partitioning of carbon associated with the bainite transformations. The appearance of martensite could be anticipated from the dilatometric measurements (Fig. 1, which showed that martensite is obtained for cooling rates as low as 0.1–0.2 $^\circ\mathrm{C\,s^{-1}}$, i.e., the rate associated with the air cooling of hot 16 mm thick plate.

6 Properties in the As–Rolled Condition

The tensile and impact properties measured for all the alloys in their hot–rolled condition are presented in Tables 2 and 3.

Of the two high–silicon Alloy 2 outperforms Alloy 1 on both the strength and toughness criteria; this is unusual because the toughness usually deteriorates when the strength increases. Furthermore, Alloy 2 also has a higher carbon concentration, which in general also leads to a decrease in impact properties.

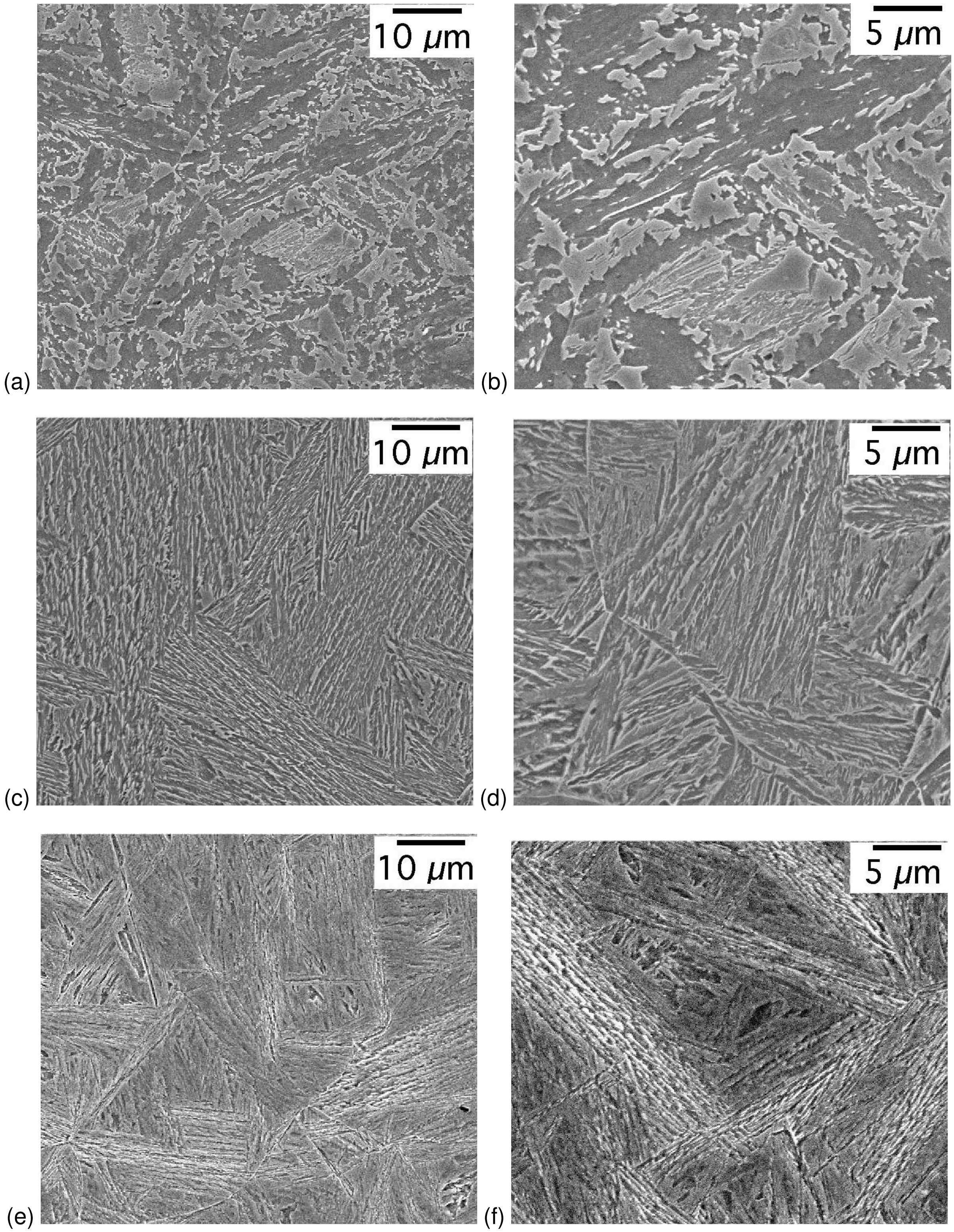

Figure 3: Scanning electron micrographs taken form the as–rolled condition. (a,b) Alloy 1, (c,d) Alloy 2, (e,f) Alloy 3.

The reason why the increase in carbon concentration has led to better mechanical properties is first that the microstructure is greatly refined by the consequent suppression of transformation temperature (Fig. 3a–d). At the same time, the suppression of transformation in Alloy 2 leads to a reduction in the amount of blocky austenite, which prevents the formation of large regions of brittle untempered martensite during the early stages of deformation. Large regions of martensite are more prone to cracking than smaller ones [47].

Table 2: Tensile test data from the hot–rolled plates.

	0.2% Proof Strength		Ultimate Tensile Strength		Proof / Ultimate
	MPa	ksi	MPa	ksi	ratio
Alloy 1	816	118	1185	172	0.69
Alloy 2	965	140	1447	210	0.67
Alloy 3	1040	151	1645	239	0.63

Table 3: Charpy impact test data from the hot–rolled plates, for V–notched 10×10 mm cross–sectioned specimens.

	Test temperature / °C	Energy Absorbed / J	% shear area
Alloy 1	24	24	25
	0	20	< 20
	-20	17	< 20
Alloy 2	24	69	100
	0	58	100
	-20	49	48
	-40	42	34
Alloy 3	24	23	25
	0	21	23
	-20	22	19

Regarding Alloy 3, the observed high strength in combination with low toughness can be directly associated to the presence of significant quantities of martensite in the as–rolled structure.

The experiments show that the best combination of mechanical properties is obtained in Alloy 2 and furthermore, the CCT diagram fro this steel shows that only minor microstructural changes are expected when the steel is cooled from austenite at rates in the range 0.15–0.30$^\circ\mathrm{C\,s^{-1}}$. These rates correspond to air–cooling of plate with thickness in the range 16–8 mm. This kind of tolerance is useful from an industrial point of view.

7 Conclusions

The alloy design and subsequent experiments show that in Si or Al–containing steels, the optimum combination of strength and toughness is associated with a fine microstructure composed of bainitic ferrite and retained austenite. As has been observed previously, blocky austenite is to be avoided.

The most promising combination of mechanical properties was obtained with Alloy 2 which in its as–rolled condition had a proof strength of 140 ksi (965 MPa), 69 Joules of impact energy at room temperature and a ductile to brittle transition temperature of $-20°$C.

However, for many high strength applications impact properties have to be improved. With this aim new steel chemistries and processing conditions are being considered, including the use of normalising and low–temperature tempering treatments.

References

[1] G. Tither and J. Kwell. Properties of directly quenched and tempered structural steel plate. *Journal of the Iron and Steel Institute*, 208:688–694, 1970.

[2] D. E. Dalton and S. Garber. Properties and structure of quenched and tempered martensitic black plate. *Journal of the Iron and Steel Institute*, 208:633–642, 1970.

[3] D. Dunne, H. Tsuei, and Z. Sterjovski. Artificial neural networks for modelling of the impact toughness of steel. *ISIJ International*, 44:1599–1607, 2004.

[4] A. Brownrigg. Why bother with heat treatment - new applications of microalloyed steels. *Metals Australasia*, 16:8–9, 1984.

[5] A. A. Gorni and P. R. Mei. Development of alternative as-rolled alloys to replace quenched and tempered steels with tensile strength in the range of 600–800 MPa. *Journal of Materials Processing Technology*, 162–163:298–303, 2005.

[6] F. G. Caballero, H. K. D. H. Bhadeshia, K. J. A. Mawella, D. G. Jones, and P. Brown. Design of novel high–strength bainitic steels: Part i. *Materials Science and Technology*, 17:512–516, 2001.

[7] F. G. Caballero, H. K. D. H. Bhadeshia, K. J. A. Mawella, D. G. Jones, and P. Brown. Design of novel high–strength bainitic steels: Part ii. *Materials Science and Technology*, 17:517–522, 2001.

[8] F. G. Caballero, M. J. Santofimia, C. Capdevila, C. Garcia-Mateo, and C. Garcia de Andrés. Design of advanced bainitic steels by optimisation of TTT diagrams and T_0 curves. *ISIJ International*, 46:1479–1488, 2006.

[9] H. K. D. H. Bhadeshia. *Bainite in Steels, 2nd edition*. Institute of Materials, London, 2001.

[10] E. C. Bain. *Alloying Elements in Steel*. American Society of Materials, Cleveland, Ohio, USA, 1939.

[11] A. G. Allten and P. Payson. The effect of silicon on the tempering of martensite. *Trans. ASM*, 45:498–532, 1953.

[12] W. S. Owen. The effect of silicon on the kinetics of tempering. *Trans. ASM*, 46:812–829, 1954.

[13] A. S. Keh and W. C. Leslie. Structure and properties of engineering materials. In *Materials Science Research*, volume 1, N. Y. USA, 1963. Plenum Publishing.

[14] J. Gordine and I. Codd. The influence of Si up to 1.5 wt% on the tempering of a spring steel. *Journal of the Iron and Steel Institute*, 207:461–467, 1969.

[15] G. W. Lorimer R. M. Hobbs and N. Ridley. Effect of silicon on the microstructure of quenched and tempered medium carbon steels. *Journal of the Iron and Steel Institute*, 210:757–764, 1972.

[16] S. J. Matas and R. F. Hehemann. The structure of bainite in hypoeutectoid steels. *TMS–AIME*, 221:179–185, 1961.

[17] R. Entin. The elementary reactions in the austenite - pearlite, bainite transformations. In V.F.Zacky and H.I.Aaronson, editors, *Decomposition of austenite by diffusional processes*, pages 295–211, New York, 1962. Interscience.

[18] J. Deliry. Noveau carbure de fer transformation bainitique dans les aciers au carbone silicium. *Memoires Scientifiques Rev. Metallurg.*, 62:527–550, 1965.

[19] J. Pomey. Revenu de la martensite et reaction bainitique inferieure: Cas des aciers au carbone-silicium et des aciers au carbone. *Memoires Scientifiques Rev. Metallurg.*, 63:507–532, 1966.

[20] R. F. Hehemann. The bainite transformation. In H. I. Aaronson and V. F. Zackay, editors, *Phase Transformations*, pages 397–432, 1970.

[21] R. Le-Houillier, G. Begin, and A. Dube. A study of the peculiarities of austenite during the bainite transformation. *Metallurgical Transactions*, 2:2645–2653, 1971.

[22] H. K. D. H. Bhadeshia and D. V. Edmonds. Bainite in silicon steels: a new composition property approach ii. *Metal Science*, 17:420–425, 1983.

[23] B. J. P. Sandvik. The bainite reaction in Fe-Si-C alloys: the primary stage. *Metallurgical Transactions*, 13A:777–787, 1982.

[24] B. J. P. Sandvik. The bainite reaction in Fe-Si-C alloys: The secondary stage. *Metallurgical & Materials Transactions A*, 13A:789–800, 1982.

[25] H. K. D. H. Bhadeshia. Advances in the kinetic theory of carbide precipitation. *Materials Science Forum*, 426–432:35–42, 2003.

[26] H. K. D. H. Bhadeshia, M. Lord, and L.-E. Svensson. Silicon–rich bainitic steel welds. *Transactions of JWRI*, 32:91–96, 2003.

[27] E. Kozeschnik and H. K. D. H. Bhadeshia. Influence of silicon on cementite precipitation in steels. *Materials Science and Technology*, 24:in press., 2008.

[28] H. K. D. H. Bhadeshia. A thermodynamic analysis of isothermal transformation diagrams. *Metal Science*, 16:159–165, 1982.

[29] H. K. D. H. Bhadeshia. The driving force for matensitic transformation in steels. *Metal Science*, 15:175–177, 1981.

[30] H. K. D. H. Bhadeshia. Thermodynamic extrapolation and the martensite-start temperature of substitutionally alloyed steels. *Metal Science*, 15:178–150, 1981.

[31] J. L. Lee and H. K. D. H. Bhadeshia. A methodology for the prediction of time-temperature-transformation diagrams. *Materials Science and Engineering A*, A171:223–230, 1993.

[32] K. J. Irvine and F. B. Pickering. High carbon bainitic steels. In *Physical properties of martensite and bainite, special report 93*, pages 110–125, London, 1965. Iron and Steel Institute.

[33] F. B. Pickering. *Physical Metallurgy and the Design of Steels*. Applied Science Publishers, Essex, U. K., 1978.

[34] F. B. Pickering. *Constitution and Properties of Steels*, pages 339–399. VCH Publishers, 1992.

[35] S. B. Singh and H. K. D. H. Bhadeshia. Estimation of bainite plate-thickness in low-alloy steels. *Materials Science and Engineering A*, A245:72–79, 1998.

[36] F. B. Pickering. Mechanism of bainite formation in low–alloy steels containing up to 0.4% carbon. In *4th International Conference on Electron Microscopy*, pages 626–637. Springer Verlag, Berlin, 1958.

[37] M. J. Roberts. Effect of transformation substructure on the strength and toughenss of fe–mn alloys. *Metallurgical Transactions*, 1:3287–3294, 1970.

[38] G. Papadimitriu and G. Fourlaris. *J. de Physique IV*, 7:C5 131–136, 1997.

[39] I. Olefjord. Temper embrittlement. *International Metals Reviews*, 4:149–163, 1989.

[40] C. L. Briant and S. K. Banerji. Intergranular failure in steel: role of grain boundary composition. *International Metals Reviews*, 4(164–199), 1978.

[41] J. S. Kirkaldy, J. von Destinon-Forstmann, and R. J. Brigham. Simulation of banding in steels. *Canadian Metallurgical Quarterly*, 59:59–81, 1962.

[42] S. A. Khan and H. K. D. H. Bhadeshia. The bainite transformation in chemically heterogeneous 300M high–strength steel. *Metallurgical Transactions A*, 21A:859–875, 1990.

[43] H. K. D. H. Bhadeshia and D. V. Edmonds. The bainite transformation in a silicon steel. *Metallurgical Transactions A*, 10A:895–907, 1979.

[44] H. K. D. H. Bhadeshia and D. V. Edmonds. The bainite transformation in a silicon steel. *Metallurgical Transactions A*, 10A:895–907, 1979.

[45] Ph. Maynier, B. Jungmann, and J. Dollet. Creusot–Loire system for the prediction of the mechanical properties of low alloy steel products. In D. V. Doane and J. S. Kirkaldy, editors, *Hardenability concepts with applications to steels*, pages 518–545, Materials Park, Ohio, USA, 1978. TMS–AIME.

[46] H. K. D. H. Bhadeshia and D. V. Edmonds. Bainite in silicon steels: a new composition property approach i. *Metal Science*, 17:411–419, 1983.

[47] S. Chatterjee and H. K. D. H. Bhadeshia. TRIP–assisted steels: cracking of high carbon martensite. *Materials Science and Technology*, 22:645–649, 2006.